2024 IEEE 100th Vehicular Technology Conference (VTC2024-Fall) | 979-8-3315-1778-6/24/$31.00 ©2024 IEEE | DOI: 10.1109/VTC2024-Fall63153.2024.10757825

Air-to-Ground Channel Modeling for UAVs in Rural Areas

Anıl Gürses
Electrical and Computer Engineering
NC State University
Raleigh, NC
agurses@ncsu.edu

Mihail L. Sichitiu
Electrical and Computer Engineering
NC State University
Raleigh, NC
mlsichit@ncsu.edu

***Abstract*—Uncrewed aerial vehicles (UAVs) have emerged as critical for various use cases, both military and civilian. This paradigm shift is poised to revolutionize various industries and aspects of modern life, from logistics and emergency services to environmental monitoring and entertainment. However, the safety of these UAVs hinges on the availability of a reliable wireless link between the UAV and the ground infrastructure for real-time communication. To effectively harness the vast potential of UAVs with safe and reliable wireless link, it is essential to model the complex air-to-ground (A2G) channel accurately. In this work, we present an open-source channel sounder built with software-defined radios (SDRs), which enables real-time measurement and characterization of the A2G channel in scenarios with mobility. Our measurement campaign conducted in a rural area provides valuable insights into the A2G channel's characteristics, multipath effects, and channel impairments. This work provides a foundation for the development of accurate A2G channel models that can be used to optimize the design and performance of UAV communication systems.**

***Index Terms*—Air-to-ground (A2G) channel, channel modeling, software-defined radios (SDRs)**

I. Introduction

As we move towards the sixth generation (6G) era, the anticipated inclusion of a broad array of advanced technologies shows a shift towards more intricate and interconnected network infrastructures. These networks are expected to integrate both aerial and non-terrestrial components [1], creating a complex mesh of technologies designed to enhance connectivity across both densely populated urban areas and remote regions. The integration of uncrewed aerial vehicles (UAVs) into these networks has many use cases, such as providing flight safety, monitoring, and surveillance, as well as enhancing the coverage of wireless networks. To this end, the characteristics of the wireless channel between the UAVs and the ground infrastructure are of paramount importance.

To optimize the design and performance of air-to-ground (A2G) communication systems, it is essential to develop accurate wireless channel models, taking into account the unique characteristics and challenges they present. Although there are various channel models available for wireless networks [2], [3], they often fail to fully capture the dynamics of the channels in A2G scenarios [4]. As an example, the 3rd Generation Partnership Project (3GPP) 38.901 [2] channel models are tailored for specific scenarios in fifth generation new radio (5G NR), such as urban macrocell (UMa), urban microcell (UMi), and rural macrocell (RMa). However, A2G channel models are not covered by any of these models. A2G channels present unique challenges due to their complex interactions with the terrestrial environment, such as obstacles, terrain irregularities, and varying atmospheric conditions. Despite the growing importance of A2G communications for UAV applications, there are no channel models for the A2G channel provided by 3GPP or other standardization bodies. There are studies that have focused on the A2G channel modeling [5]–[7] for different scenarios. However, these studies rely on solutions that are not publicly available such as commercial channel sounders, which are not easily accessible or customizable by others. Some studies have used signals like LTE for A2G channel measurements [6], but these signals are not always available in the desired frequency bands and are limited to certain bandwidths.

In this work, we address this gap by presenting an open-source channel sounder and A2G channel measurement campaign in rural areas to understand the dynamics of the A2G channel. Our contributions are as follows:

- We present an open-source channel sounder built using software-defined radios (SDRs), specifically universal software radio peripherals (USRPs), to measure the A2G channel.
- We use the developed channel sounder in conjunction with a UAV to gather experimental data.
- We analyze the measurement results and show that traditional statistical models, such as the log-normal shadowing model and the 3GPP 38.901 RMa, do not adequately capture the complex dynamics of the A2G channels.

II. Background and System Overview

A. Channel Models

The channel models should capture the characteristics of the wireless channel, such as path loss and shadowing. Path loss is a major component of the channel model, which is defined as the decrease in the signal strength as a function of

This work was supported in part by the NSF PAWR Program under Grant CNS-193933.

distance between the transmitter and receiver. Shadowing is another important component, which is caused by the obstacles between the transmitter and receiver, such as buildings, trees, and terrain. Fading is the rapid fluctuation of the signal strength due to the multipath propagation, which is caused by the reflections, diffractions, and scattering of the signal. These components are generally captured by statistical models, such as the log-normal shadowing and the 3GPP channel models [2].

1) Log-distance Path Loss Model: One of the most commonly used path loss models is the log-distance path loss model, which is based on the Friis transmission equation. Log-distance path loss model can be expressed as follows:

$$L(d) = L_0 + 10\gamma \log_{10}\left(\frac{d}{d_0}\right) + X_\sigma. \quad (1)$$

where L_0 is the path loss in dB at a reference distance d_0, γ is the path loss exponent, which depends on the specific propagation environment, d_0 is the reference distance, and X_σ is the log-normal shadowing with standard deviation σ.

2) 3GPP RMa Path Loss Model: The 3GPP RMa path loss model is an example of a statistical model that is applicable to rural environments. It provides a detailed representation of path loss as a function of various factors, including distance, frequency, and antenna positions. The RMa line-of-sight (LOS) path loss model [2] is defined as:

$$PL_{\text{RMa-LOS}}(d_{3D}) = \begin{cases} PL_1, & 10m \le d_{2D} \le d_{BP} \\ PL_2, & d_{BP} < d_{2D} \le 10km \end{cases}, \quad (2)$$

where d_{2D} is the 2D distance (horizontal projection), d_{3D} is the 3D distance (actual propagation distance), and d_{BP} is the breakpoint distance beyond which diffraction becomes the dominant propagation mechanism. The values for PL_1 and PL_2 are calculated as follows:

$$\begin{aligned} PL_1 = {} & 20\log_{10}(40\pi d_{3D} f_c/3) \\ & + \min(0.03 h_{\text{BS}}^{1.72}, 10)\log_{10}(d_{3D}) \\ & + \min(0.044 h_{\text{BS}}^{1.72}, 14.77) \\ & - 0.002\log_{10}(h_{\text{BS}}) d_{3D} \end{aligned} \quad (3)$$

$$PL_2 = PL(d_{BP}) + 40\log_{10}(d_{3D}/d_{BP}), \quad (4)$$

with f_c representing the carrier frequency in GHz, h_{BS} as the base station antenna height, and h_{UT} as the user terminal antenna height. The standard deviation of shadow fading is denoted as σ_{SF} with various values depending on the environment.

B. Channel Sounder

Channel sounders are special tools used for measuring and characterizing wireless channels by transmitting a known signal with certain properties and estimating the characteristics of the channel from the received signal. This process is crucial for understanding and modeling the behavior of wireless channels under different conditions, which is essential for the development and optimization of wireless communication systems.

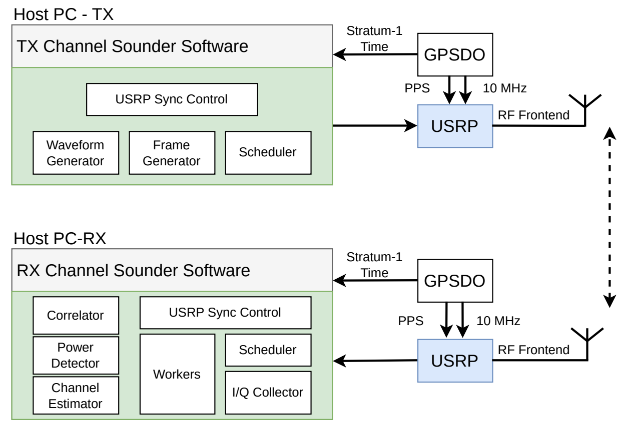

Fig. 1: Channel sounder system overview.

There are several approaches to design a channel sounder, such as vector network analyzer (VNA)-based and software-defined radio (SDR)-based channel sounders. VNA-based sounders [8] are particularly effective in controlled environments where precise measurements are critical. They typically excel in laboratory settings where stable and repeatable measurements are crucial. However, VNAs are generally less adaptable to mobile or field scenarios due to their size and complexity. In contrast, SDR-based channel sounders [9] offer greater flexibility and are capable of operating over a wide range of frequencies and conditions. They are particularly valued for their adaptability in field tests and dynamic environments, where conditions can change rapidly.

Although channel sounders are straightforward in concept, they require careful attention to several technical details to ensure accurate measurements. These details include time and clock synchronization, power calibration, and antenna calibration. Time and clock synchronization are pivotal in guarantee that the transmitter and receiver operate concurrently, with their local oscillators aligned in both frequency and time. This synchronization ensures accurate timing of the signal transmission and reception, which is critical for capturing the channel impulse response and other channel metrics. Furthermore, power calibration is essential to ensure that the transmitted and received signal levels are accurately captured so path loss and signal strength measurements are reliable and repeatable. Moreover, antenna calibration is necessary to account for the non-uniformity of the antenna gain. In this study, antenna calibration is achieved through the measurements obtained from the following study [10]. Each of these factors is vital for the reliable operation of channel sounders and the validity of the data they produce.

In this work, we propose an open-source channel sounder based on USRP, which is capable of measuring the channel characteristics in real-time with different waveform con-

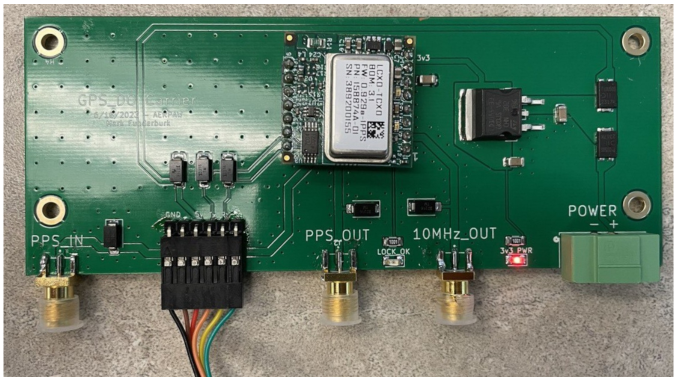

Fig. 2: The custom built GNSS-DO board.

figurations, such as frequency-modulated continuous wave (FMCW), Zadoff-Chu (ZC), and pseudo-noise (PN) sequence. The proposed channel sounder is capable of measuring path-loss, channel impulse response (CIR), time-of-flight (ToF), power delay profile, and doppler shift, which are essential for understanding the wireless channel characteristics. The system is designed to be portable and flexible, making it suitable for field tests and mobile scenarios. As shown in Figure 1, the system consists of three components: 1) USRP SDR, 2) GNSS-disciplined oscillator (GNSS-DO) board for synchronization, and 3) a host PC for data processing. The sounder software keeps track of the synchronization during the measurement process, which ensures that the transmitted and received signals are aligned in time and frequency. The time synchronization is tightly coupled with the scheduler, which ensures that the transmitted signal is sent at a preestablished time, and the received signal is captured at the same time.

Channel sounder's measurement is verified through a closed loopback measurement system, where the transmit port is directly connected to the receive port through a loopback channel that is generated by a diplexer that involves two cables of different lengths to create two distinct paths. Additionally, the system is calibrated for RF power, which ensures that the path loss and received signal power are accurately measured.

The GNSS-DO board is used for providing time and frequency synchronization between the transmitter and receiver radios. Although internal GPS-disciplined oscillators (GPSDO) are available for USRP, they are not capable of providing the required synchronization accuracy for high bandwidth channel measurements. In this work, we developed an external GNSS-DO board (as shown in Figure 2), which is capable of providing a stable 10 MHz clock signal with a 2.5 ns accuracy in time. The custom designed GNSS-DO board includes two components; a GNSS receiver and an external temperature-compensated crystal oscillator (TCXO) with a PLL, which ensures stability over the measurement. The GNSS receiver provides a pulse-per-second (PPS) with 2.5 ns accuracy in time, where the PLL of the TCXO uses this input signal to tune into the GNSS PPS and provide a reliable 10 MHz clock signal. PPS and reference 10 MHz signals are then fed into the USRP for absolute time and frequency synchronization of the transmitter and receiver.

The stability of GNSS is enhanced with real-time kinematics (RTK), where the RTK base station is located at the fixed node. RTK base station provides radio technical commission for maritime services (RTCM) corrections to the GNSS receiver, which improves the accuracy of the GNSS signal. This leads to more accurate location information and time synchronization for the measurements.

The channel sounder captures the channel by using the sliding correlation principle [11], which uses the cross-correlation of the transmitted and received signals to estimate the channel impulse response. The transmitted signal is known at the receiver, and it has a known structure with low autocorrelation sidelobes.

Although the channel sounder featured multiple waveforms, for this work we used the ZC sequence as the transmitted signal, which has a low autocorrelation property and is widely used in channel sounders [12]. The ZC sequence is defined as:

$$x[n] = e^{-j\frac{\pi r n(n+1)}{N}} \tag{5}$$

where n ranges from 0 to $N-1$, r is the root index, and N is the length of the sequence which is relatively prime to r.

The transmitted signal is sent as a burst, where the transmitter sends a frame with multiple ZC sequences with a guard period between each sequence. The first ZC sequence is transmitted at the rise of the PPS signal while the receiver only captures signal-of-interest for the duration of the sequence with paddings on the front and back, which makes storing and processing efficient. There can be more than one frame per second, and the ZC sequence is repeated multiple times in each frame. This ensures that the channel characteristics are captured in both short and long time interval configurations. We model the received signal as:

$$r(t) = h(t) * s(t) + n(t) \tag{6}$$

where $h(t)$ is the CIR, $s(t)$ is the transmitted signal, and $n(t)$ is the noise. The CIR, $h[\tau]$, in discrete time can be estimated using the sliding correlation between the received signal $r[n]$ and the time-shifted conjugate of the transmitted signal $s[n]$, defined as:

$$h[\tau] = \sum_{n=-\infty}^{\infty} r[n]s^*[n-\tau] \tag{7}$$

where $s^*[n-\tau]$ is the complex conjugate of $s[n]$ shifted by τ.

Path loss can be estimated both from the CIR and the received signal power,

$$L_{meas} = \frac{P_t}{P_r} = -10\log_{10}\sum |h[n]|^2 \tag{8}$$

where P_t is the transmitted power and P_r is the received power. Since both the transmit and receiver reference power levels at the TX and RX USRPs are known (measured at the calibration step) the path loss can be calculated directly from the received power level.

Fig. 3: The UAV and portable node used for the measurements.

Fig. 4: The UAV during flight and fixed node (tower).

III. Experiment Results

A. Measurement Setup

To measure the A2G channel, we conducted nine flights using the developed channel sounder in conjunction with a UAV, as shown in Figure 3. In the measurements, a custom built UAV (hexacopter) from Aerial Experimentation and Research Platform for Advanced Wireless (AERPAW) testbed [13] is used, which is equipped with a portable node that includes the USRP B210, GNSS-DO board, and Intel NUC as a host PC for radio and vehicle control [14]. The portable node that is mounted on the UAV is used as the receiver, while the fixed node is used as the transmitter. The fixed node, shown in Figure 4, is a tower with a 10 m height with USRP B210, a GNSS-DO board, and a server for data processing.

USRP B210 is capable of transmitting and receiving signals up to 6 GHz with 56 MHz bandwidth. Although the developed channel sounder is capable of handling more advanced USRPs, we used USRP B210 on both ends for our measurements due to its portability. Measurements are taken at 56 MHz bandwidth, which is the maximum bandwidth that USRP B210 can handle.

Each flight was carefully planned at three altitudes and three frequencies within the Citizens Broadband Radio Service (CBRS) band. These variations were strategically chosen to explore and understand how different flight altitudes and signal frequencies influence the dynamics of the A2G communication channel. The specific altitudes and parameters used during these tests are detailed in Table I. The specific frequencies were chosen to be free from in channel and side channel interference at the time of the measurements.

The measurements are conducted in AERPAW testbed [13], a rural area with minimal interference and few obstacles, which allows us to focus on the A2G channel characteristics. Initiating the study in such a straightforward environment allows for a clearer understanding of the A2G channel dynamics before introducing the complexities of more urban or obstructed settings. For the purposes of this study, the UAV is flown at a constant speed of 5 m/s along a straight path of 500

Parameter	Value
Center Frequency	3564, 3620, 3686 MHz
Sampling Rate	56 MHz
Transmit Power	19 dBm
Transmitted Waveform	Zadoff-Chu Sequence
Sequence Length	401
Root index	200
Repetition of Sequence	4
Measurement Frequency	4 Hz
Altitude (above ground level)	30, 60, 90 m
Flight Speed	5 m/s
Flight Path	500 m

TABLE I: Measurement Parameters

Fig. 5: The three flight paths of the UAV at constant altitudes of 30m, 60m, and 90m above ground level at the starting location.

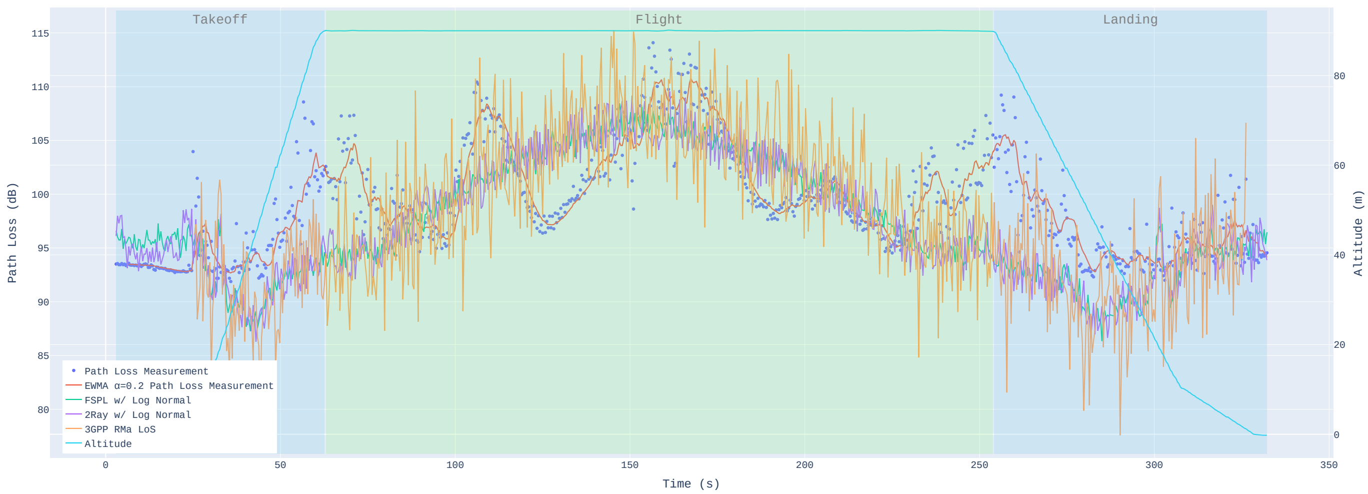

Fig. 6: Path loss values from measurement and available statistical models at 90m, 3620 MHz.

Fig. 7: Received signal power values over distance at different altitudes and frequencies.

m, as shown in Figure 5. Over the flight path, the yaw of the UAV is kept constant (i.e., it was facing North the entire flight). This stability in orientation is critical as it minimizes any potential impact that changes in antenna orientation might have on the measurement accuracy, thereby ensuring the reliability of the data collected.

B. Measurements and Results

Figure 6 illustrates the path loss measurements taken at an altitude of 60 meters and a center frequency of 3620 MHz, showing the path loss as a function of time. In addition to empirical measurements, Figure 6 also presents reference statistical path loss models for comparative analysis. These include the free space path loss model, the two-ray model with log-normal shadowing, and the 3GPP 38.901 RMa model. The log-normal shadowing is generated from the distribution of the measurement data, while the 3GPP 38.901 RMa shadowing is generated using the parameters provided in the standard. Antenna patterns, which are acquired from measurements in an anechoic chamber, are also considered in the analysis

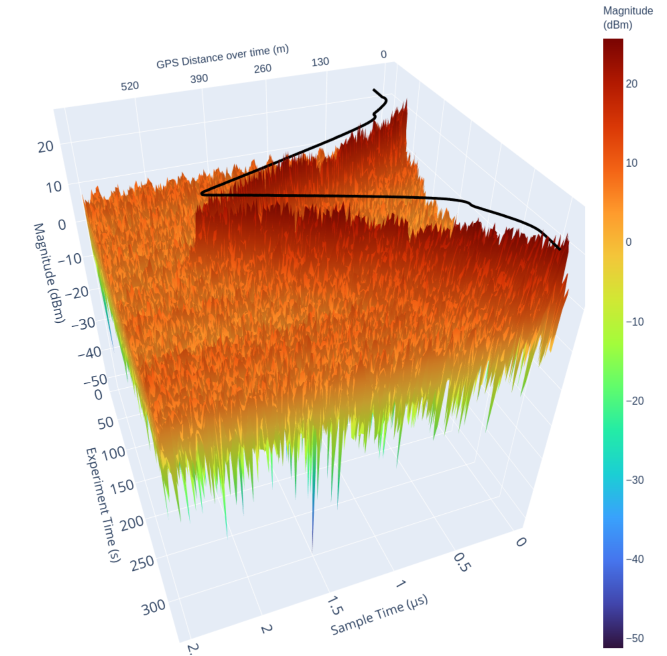

Fig. 8: Channel impulse response over the flight at 90 m altitude, 3620 MHz center frequency.

to account for the directional characteristics of the antennas used in the measurements and any additional losses that may occur due to the antenna orientation. Although the direction-of-arrival (DoA) is calculated from GPS coordinates, it is assumed that DoA is not spread over a wide range, which is a reasonable assumption for rural area.

The measurements show that the path loss is not monotonic as a function of the distance, which is expected due to the mobility of the UAV, the varying terrain, and fading. In Figure 7, the received signal power values are shown over distances at different altitudes and frequencies with exponentially weighted moving average (EWMA). Despite the relatively flat terrain, there are significant fluctuations in path loss and received signal power, underscoring a discrepancy between observed data and the predictions made by existing statistical models.

Figure 8 shows the channel impulse response of the received signal over the flight at 90 m altitude and 3620 MHz center frequency. The black line shows the delay corresponding to the physical distance between the UAV and the fixed node, which increases as the UAV moves away from the fixed node. The CIR is estimated using the sliding correlation principle, which captures the channel dynamics over time. As shown in Figure 8, the delay tap increases as the UAV moves away from the fixed node, which shows that the PPS synchronization is working correctly. The variations observed in the path loss and received signal power are also reflected in the CIR, which shows the rapid changes in the channel conditions due to the mobility of the UAV and the varying terrain. Reflections are not that strong in the CIR, which is expected due to the relatively flat terrain and the absence of obstacles. However, the CIR shows that there are reflections and multipath components in the channel, which are relatively at closer distances.

IV. Conclusion

In this paper, we presented a novel open-source SDR-based channel sounder system and A2G channel measurement results that has been obtained from a rural area with a UAV, specifically AERPAW testbed. Measurements show that the A2G channel is dynamic and complex, with rapid changes in path loss and shadowing which is not captured by the statistical models available today. Channel sounder code and the measurement data are available at [15].

References

[1] G. Geraci, A. Garcia-Rodriguez, M. M. Azari, A. Lozano, M. Mezzavilla, S. Chatzinotas, Y. Chen, S. Rangan, and M. Di Renzo, "What will the future of uav cellular communications be? a flight from 5G to 6G," *IEEE communications surveys & tutorials*, vol. 24, no. 3, pp. 1304–1335, 2022.

[2] "Study on channel model for frequencies from 0.5 to 100 GHz," 3rd Generation Partnership Project (3GPP), Technical Specification 38.901, June 2020, version 16.1.0. [Online]. Available: https://www.3gpp.org/DynaReport/38901.htm

[3] P. KYOSTI, "WINNER II channel models," *IST, Tech. Rep. IST-4-027756 WINNER II D1.1.2 V1.2*, 2007. [Online]. Available: https://cir.nii.ac.jp/crid/1571698600936523008

[4] T. S. Rappaport, S. Sun, and M. Shafi, "Investigation and comparison of 3GPP and NYUSIM channel models for 5G wireless communications," in *2017 IEEE 86th Vehicular Technology Conference (VTC-Fall)*, 2017, pp. 1–5.

[5] R. Sun and D. W. Matolak, "Air–ground channel characterization for unmanned aircraft systems part II: Hilly and mountainous settings," *IEEE Transactions on Vehicular Technology*, vol. 66, no. 3, pp. 1913–1925, 2017.

[6] X. Cai, J. Rodríguez-Piñeiro, X. Yin, N. Wang, B. Ai, G. F. Pedersen, and A. P. Yuste, "An empirical air-to-ground channel model based on passive measurements in LTE," *IEEE Transactions on Vehicular Technology*, vol. 68, no. 2, pp. 1140–1154, 2019.

[7] M. U. Akram, U. Saeed, S. A. Hassan, and H. Jung, "UAV-based air-to-ground channel modeling for diverse environments," in *2020 IEEE Wireless Communications and Networking Conference (WCNC)*, 2020, pp. 1–6.

[8] J. Hejselbaek, W. Fan, and G. F. Pedersen, "Ultrawideband VNA based channel sounding system for centimetre and millimetre wave bands," in *2016 IEEE 27th Annual International Symposium on Personal, Indoor, and Mobile Radio Communications (PIMRC)*. IEEE, 2016, pp. 1–6.

[9] J. Huang, Y. Liu, C.-X. Wang, J. Sun, and H. Xiao, "5G millimeter wave channel sounders, measurements, and models: Recent developments and future challenges," *IEEE Communications Magazine*, vol. 57, no. 1, pp. 138–145, 2019.

[10] S. J. Maeng, O. Ozdemir, I. Guvenc, and M. Sichitiu, "3D antenna pattern measurement for AERPAW experiments," 2023. [Online]. Available: https://dx.doi.org/10.21227/mma2-0t93

[11] R. J. Pirkl and G. D. Durgin, "Optimal sliding correlator channel sounder design," *IEEE Transactions on Wireless Communications*, vol. 7, no. 9, pp. 3488–3497, 2008.

[12] E. Kassem, R. Marsalek, and J. Blumenstein, "Frequency domain Zadoff-Chu sounding technique for USRPs," in *2018 25th International Conference on Telecommunications (ICT)*. IEEE, 2018, pp. 302–306.

[13] AERPAW, "Aerial Experimentation and Research Platform for Advanced Wireless," 2024. [Online]. Available: https://aerpaw.org/

[14] M. Funderburk, J. Kesler, K. Sridhar, M. L. Sichitiu, I. Guvenc, R. Dutta, T. Zajkowski, and V. Marojevic, "AERPAW vehicles: Hardware and software choices," in *Proceedings of the Eighth Workshop on Micro Aerial Vehicle Networks, Systems, and Applications*, ser. DroNet '22. New York, NY, USA: Association for Computing Machinery, 2022, p. 37–42.

[15] "USRP-Channel-Sounder," GitHub repository. [Online]. Available: https://github.com/anilgurses/USRP-Channel-Sounder